The root endophytic fungus *Piriformospora indica* requires host cell death for proliferation during mutualistic symbiosis with barley

Sachin Deshmukh*, Ralph Hückelhoven*†, Patrick Schäfer*, Jafargholi Imani*, Monica Sharma*, Michael Weiss‡, Frank Waller*, and Karl-Heinz Kogel*§

*Research Centre for Biosystems, Land Use, and Nutrition, Institute of Phytopathology and Applied Zoology, Justus Liebig Universität, D-35392 Giessen, Germany; †Institute of Phytopathology, Technische Universität München, D-85350 Freising, Germany; and ‡Institute of Systematic Botany and Mycology, Eberhard Karls Universität, D-72076 Tübingen, Germany

Fungi of the recently defined order Sebacinales (Basidiomycota) are involved in a wide spectrum of mutualistic symbioses (including mycorrhizae) with various plants, thereby exhibiting a unique potential for biocontrol strategies. The axenically cultivable root endophyte *Piriformospora indica* is a model organism of this fungal order. It is able to increase biomass and grain yield of crop plants. In barley, the endophyte induces local and systemic resistance to fungal diseases and to abiotic stress. To elucidate the lifestyle of *P. indica*, we analyzed its symbiotic interaction and endophytic development in barley roots. We found that fungal colonization increases with root tissue maturation. The root tip meristem showed no colonization, and the elongation zone showed mainly intercellular colonization. In contrast, the differentiation zone was heavily infested by inter- and intracellular hyphae and intracellular chlamydospores. The majority of hyphae were present in dead rhizodermal and cortical cells that became completely filled with chlamydospores. In some cases, hyphae penetrated cells and built a meshwork around plasmolyzed protoplasts, suggesting that the fungus either actively kills cells or senses cells undergoing endogenous programmed cell death. Seven days after inoculation, expression of barley *BAX inhibitor-1* (*HvBI-1*), a gene capable of inhibiting plant cell death, was attenuated. Consistently, fungal proliferation was strongly inhibited in transgenic barley overexpressing GFP-tagged HvBI-1, which shows that *P. indica* requires host cell death for proliferation in differentiated barley roots. We suggest that the endophyte interferes with the host cell death program to form a mutualistic interaction with plants.

biodiversity | mycorrhiza | rhizosphere | Sebacinales | systemic resistance

Most plants studied in natural ecosystems are infested by fungi that cause no disease symptoms. These endophytic fungi are distinguished from pathogens that lead to disease and reduce the fitness of their host plants (1). In many cases, endophytes form mutualistic interactions with their host, the relationship therefore being beneficial for both partners. Mutualism frequently leads to enhanced growth of the host. The beneficial effects for the plant can be a result of an improved nutrient supply by the endophyte as known for arbuscular mycorrhizal symbiosis, the most intensely studied mutualistic plant–fungus interaction (2). In addition to providing mineral nutrients, endophytes also can improve plant resistance to pathogens as demonstrated for arbuscular mycorrhiza fungi (AMF) in roots (3) and for a highly diverse spectrum of ascomycete endophytes in leaves (4, 5).

Mutualism requires a sophisticated balance between the defense responses of the plant and the nutrient demand of the endophyte. Hence, a mutualistic interaction does not imply absence of plant defense. Defense-related gene expression has been well studied during host colonization by obligate biotrophic AMF. Induction of defense genes was most prominent at early time points during penetration (6) but could also be detected during arbuscule development (7). On the other hand, there is clear evidence for impeded defense reactions during the establishment of mycorrhization. It is therefore a rather fine-tuned balance that keeps a mutualistic interaction in a steady state without disadvantages for both partners (8).

In the present work we aimed at studying fungal development and host reactions in the mutualistic symbiosis of the fungal root endophyte *Piriformospora indica* and barley (9, 10). The basidiomycete is a model organism for species of the recently described order Sebacinales, fungi that are involved in a uniquely wide spectrum of mutualistic symbioses (mycorrhizae) with plants (11). The axenically cultivable *P. indica* increases biomass and grain yield of crop plants. In barley, the endophyte induces root resistance against *Fusarium culmorum*, one of the fungal species causing head blight, and systemic resistance to barley powdery mildew *Blumeria graminis* f.sp. *hordei* via an unknown mechanism probably independent of salicylate or jasmonate accumulation. Moreover, *P. indica* protects barley from abiotic stress, such as high salt concentrations (10).

P. indica was originally discovered in the Indian Thar desert in northwest Rajasthan. *In vitro* experiments have shown a broad host spectrum of the fungus (12), including members of the Brassicaceae, like *Arabidopsis*, which are not colonized by AMF. As in barley, *P. indica* enhances seed yield, reduces the time for seed ripening, and increases tolerance to abiotic stress in *Arabidopsis* (13). How the fungus penetrates plant roots, how roots are eventually colonized, or whether the mutualistic fungus has a facultative biotrophic or a necrotrophic lifestyle are issues that have not yet been studied. In *Arabidopsis*, mycelium covers the surface of the roots. Hyphae penetrate root hairs and rhizodermis cells and eventually form chlamydospores in these cells (13). Our previous observations in barley revealed that the fungus, in contrast to obligate biotrophic AMF, colonizes dead root cells, suggesting a previously uncharacterized type of mutualism. Here

Fig. 1. Phylogenetic placement of the strains tested in this study within the Sebacinales, estimated by maximum likelihood from an alignment of nuclear rDNA coding for the 5' terminal domain of the ribosomal large subunit. Branch support is given by nonparametric maximum likelihood bootstrap (first numbers) and by posterior probabilities estimated by Bayesian Markov chain Monte Carlo (second numbers). Support values of <50% are omitted or indicated by an asterisk. The tree was rooted according to the results of ref. 11, and subgroups discussed in ref. 11 are denoted with ''A'' and ''B.'' Sequences of the strains used in this study are indicated by black circles. Sequences from morphologically determined specimens or cultures are printed in bold. Sebacinalean sequences obtained from mycorrhizal plant roots are assigned to mycorrhizal types by the following acronyms: CVM, cavendishioid mycorrhiza (14); ECM, ectomycorrhiza; ERM, ericoid mycorrhiza; JMM, jungermannioid mycorrhiza; and ORM, orchid mycorrhiza. Proveniences are given as follows: A, Austria; AUS, Australia; CAN, Canada; CHN, People's Republic of China; ECU, Ecuador; EST, Estonia; FRA, France; GER, Germany; GUY, Guyana; IND, India; MEX, Mexico; NOR, Norway; and SPA, Spain.

we provide cytological and molecular evidence that *P. indica* proliferates in dead host cells and that colonization gradually increases with tissue maturation. The expression level of the cell death regulator *BAX inhibitor-1* (*HvBI-1*) appears critical for *P. indica* development in barley, suggesting that the recently discovered endophyte interferes with the host cell death machinery.

Results

P. indica Belongs to the Recently Defined Order Sebacinales. Based on the nuclear genes coding for the large ribosomal subunit (nucLSU), available strains of the *Sebacina vermifera* species complex (Sebacinales group B) are closely related to *P. indica* (Fig. 1). We addressed the question whether strains of the *S. vermifera* complex exhibit comparable biological activities as *P. indica*. To this end, barley seedlings were inoculated with *P. indica* or different isolates of *S. vermifera* and shoot length and biomass were determined (Table 1). Despite obvious variation, we found consistent biological activities in the same order of magnitude as with *P. indica*. To determine the potential for systemic induction of resistance, barley third leaves from endophyte-colonized and noncolonized, 21-day-old plants were inoculated with the conidia of *B. graminis* f.sp. *hordei*, and powdery mildew pustules were counted after 7 days. We found consistent resistance-inducing activity of all strains of the *S. vermifera* complex, although there was considerable variation of the fungal activity of the different isolates (Table 1). These data support the view that the order Sebacinales is a source of endophytes with a feasible agronomical impact.

Endophytic Development in Barley Roots. To track endophytic development in barley, root penetration and colonization were analyzed by fluorescence microscopy. In general, we observed a gradual increase of fungal colonization and proliferation associated with root maturation (Fig. 2a). Colonization initiates from chlamydospores, which, upon germination, finally form a hyphal network on and inside the root. Hyphae enter the subepidermal layer through intercellular spaces where they branch and continue to grow (Fig. 2 b–e). In young differentiated root tissue, the fungus then often colonizes and completely fills up single cells (Fig. 2 f and g) before adjacent cells are colonized, whereas an unrestricted net-like intra- and intercellular colonization pattern is observed in mature parts. Intracellular growing hyphae show necks at sites where the fungus traverses a cell wall (Fig. 2h). Occasionally, subepidermal hyphae penetrate the space between the cell wall and plasma membrane of rhizodermal or cortical cells. After branching, these hyphae enwrapped protoplasts, which showed cytoplasmic shrinkage (Fig. 3a). At later colonization stages, fungal hyphae excessively occupied rhizodermal and cortical cells. In some cases, transverse cell walls of adjoining cortical cells were absent, with the protoplasts covered by a dense meshwork of fungal hyphae. Eventually arrays of single spores developed from intracellular hyphal tips (Fig. 3 b and c). The fungus also penetrated basal parts of root hair cells, in which branching hyphae form large numbers of chlamydospores starting from the base of the root hair until a stack of spores fills the root hair (data not shown). In addition to this intracellular spore

Table 1. Effect of different Sebacinales species on barley biomass and systemic resistance to powdery mildew

Species/isolate	Increase in shoot length, %	Increase in shoot fresh weight, %	Reduction in leaf infection by *B. graminis*, %
P. indica	13.66**	26.45**	70.85**
S. v./MAFF305830	23.25**	48.24**	79.45**
S. v./MAFF305842	16.87**	15.48*	56.36*
Multinucleate *Rhizoctonia*/DAR29830	7.56**	10.76*	56.27*
S. v./MAFF305828	14.97**	28.72**	10.89
S. v./MAFF305837	16.34**	32.01**	58.19**
S. v./MAFF305835	7.80*	9.82	50.74*
S. v./MAFF305838	7.72**	6.41	44.89*

Species/isolates are shown with their culture collection numbers. Isolates of *Sebacina vermifera* (*S. v.*) were obtained from the National Institute of Agrobiological Sciences (Tsukuba, Japan); the isolate DAR29830 was kindly provided by Karl-Heinz Rexer (University of Marburg, Marburg, Germany). Values are means of three independent experiments, each consisting of 60 endophyte-inoculated and mock-inoculated plants, respectively. Powdery mildew infection was calculated from the number of fungal colonies developing on third leaf segments 7 dai with *B. graminis* f.sp. *hordei,* race A6 (15). Asterisks denote statistically significant differences between the respective values of endophyte-colonized and noncolonized plants (*, $P < 0.05$, Student's *t* test; **, $P < 0.01$, Student's *t* test).

formation, chlamydospores also were generated in the mycelial mats at the root surface.

***P. indica* Proliferates in Dead Cells.** We addressed the question of whether cortical and rhizodermal cells heavily occupied by fungal hyphae and chlamydospores were alive. In a cell viability assay with the fluorescent marker fluorescein diacetate, colonized cells did not show enhanced green fluorescence, suggesting that they were dead. In addition, these cells did not show any visible cytoplasmic streaming. Staining of colonized root hairs with an Alexa Fluor-488-labeled anti-actin antibody failed to show any host cytoskeleton, whereas noncolonized root hairs showed intact actin filaments (data not shown). To confirm that fungal colonization associates with dead cells, we double-stained root segments with DAPI for intact plant nuclei and wheat germ agglutinin-Alexa Fluor 488 (WGA-AF 488) for fungal chitin. We found a close spatial association of strong fungal colonization (Fig. 3 *d* and *f*) and DAPI-negative cells (Fig. 3 *e* and *g*), further suggesting that massive development of *P. indica* takes place in dead host cells.

Microscopic analyses demonstrated a fungal colonization pattern that strongly associated with the developmental stage of the host tissue (Fig. 2*a*). To substantiate this finding, we determined the amount of *P. indica* in different root zones by quantitative PCR using *P. indica* genomic DNA as a template for the quantification of the *P. indica* translation elongation factor gene *Tef* relative to the plant ubiquitin gene. Ten days after inoculation, the roots were cut into 0.5-cm-long apical segments of the root tip with the root cap and a basipetal segment including the differentiation zone. Consistent with the cytological data, we found a 5-fold higher relative amount of *P. indica* in the differentiation zone as compared with the apical root segment (2.53 ± 0.23 compared with 0.52 ± 0.12).

Analysis of fungal growth in the apical elongation zone revealed fungal development in intercellular spaces and formation of subepidermal intercellular hyphal mats. In contrast to its development in the differentiation zone, neither host cell wall degradation nor heavy fungal sporulation could be observed in this tissue, supporting the notion that there is a correlation between root tissue and fungal development. Juvenile tissue, which is considered to display less developmental cell death, is thus less occupied by *P. indica*. To support this observation, we tested for genomic DNA fragmentation by probing gel blots of high-molecular-weight DNA isolated from different root seg-

ments with radioactively labeled DNA probes. Genomic DNA fragmentation results from programmed cell death (PCD). As expected, the proportion of low-molecular-weight DNA fragments resulting from DNA fragmentation was lower in root tips than in mature parts of the root. *P. indica* did not change the amount of DNA fragmentation in root tips, whereas a small increase of 5–9% low-molecular-weight DNA was detected in the mature zone 10 days after inoculation with *P. indica*. To visualize DNA fragmentation in the root tissue, we used *in situ* DNA nick-end labeling and observed DNA fragmentation in nuclei of protoplasts enwrapped by *P. indica* (Fig. 3*h*). However, this was a rare event perhaps indicating a transient status before nuclei completely dissolved in invaded cells. Taken together, these results indicate that invasive growth of *P. indica* mainly occupies dead and dying cells in barley roots. Consistently, the fungus infested only dead cells of the root cap at the root tip zone, whereas the central meristematic tissue was always free of fungal hyphae (Fig. 3*i*). In adjacent cortical tissue, the fungus was present in the intercellular spaces of cells differentiating into cortical and epidermal tissue apparently without affecting differentiation. Accordingly, lateral root development from cambial cells that differentiate in root tip meristems was not compromised in roots infested by *P. indica*.

We measured the ratio of fungus to plant DNA (fungus/plant DNA ratio, FPDR) over time to check whether *P. indica* overgrows barley roots at late interaction stages. We observed an early moderate increase of the FPDR (1.8-fold) followed by a decrease and a final steady state (data not shown). This pattern reflects the symbiotic interaction in which the fungus develops moderately, subsequently induces plant growth (reflected in a decrease of FPDR), and finally reaches a steady-state level of fungal structures in the plant root. This growth pattern indicates a final balance of root growth and fungal proliferation.

Balancing of Host Cell Death and Impact of the Cell Death Regulator BAX Inhibitor-1. Because the cytological analysis of root colonization suggested that *P. indica* proliferates in dead host cells, we addressed the question of whether root invasion by *P. indica* interferes with the host's cell death machinery. Therefore, we kinetically analyzed expression of barley *HvBI-1*. BI-1 is one of the few conserved cell death suppressor proteins that apparently controls PCD in all eukaryotes and is considered a regulator of endoplasmic reticulum-linked Ca^{2+} signaling. In plants, *BI-1* is often activated in response to biotic or abiotic stresses (15–17).
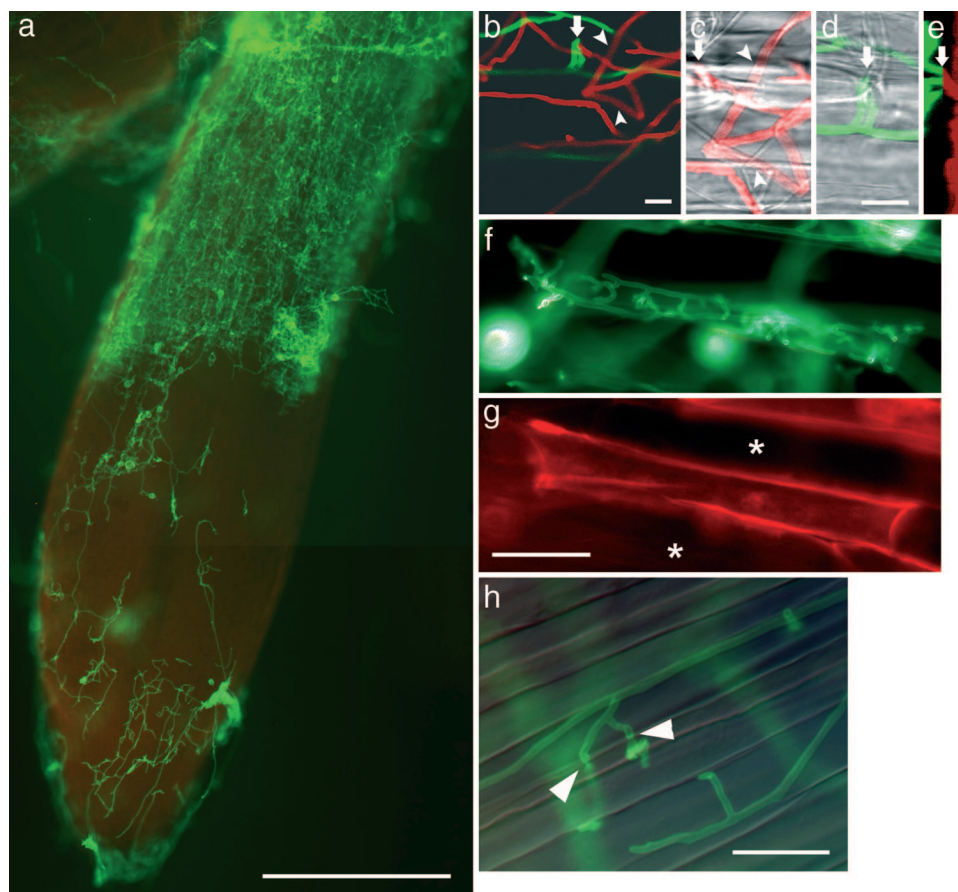
Fig. 2. Infestation pattern of *P. indica* in barley roots. (*a*) By 8 dai, hyphae excessively occupy rhizodermal and cortical cells of the differentiation zone. The elongation zone is less colonized, with occasional intercellular subepidermal hyphal structures. The root cap is heavily infested with hyphae. (*b–e*) After penetration (arrows) fungal hyphae colonize the subepidermal layer. (*b*) To better visualize the position of hyphae in the *z* axis, a confocal laser scanning image consisting of 30 frames of adjacent focal planes (*z* axis) was displayed as a maximum projection with the fluorescent signal of the wheat germ agglutinin-stained fungal hyphae displayed in red for the upper (abaxial) 15 frames and in green for the lower (adaxial, subepidermal) 15 frames. (*c* and *d*) For visualization of plant cell walls, two close-up bright-field images of two different focal planes are superimposed with the respective frames of the fluorescence images. Intercellular hyphae start branching and proliferate within the subepidermal space. (*c*) Subepidermal hyphae crossing cell walls (arrowheads) without exhibiting morphological changes (e.g., neck formation, as in *h*) revealing their periclinal localization. (*d*) The upper focal plane is characterized by hyphae penetrating the anticlinal space of adjacent rhizodermis cells. (*e*) Projection of the fluorescent signals of *c* and *d* in the *y* axis (vertical) and *z* axis (horizontal). Absence of fluorescent signals between adaxial (green) and abaxial hyphae (red) indicates a layer of rhizodermal cells free from hyphae. The penetration site is indicated by an arrow. (*f*) Colonization of a cell within young differentiated tissue. After penetration, the cell is completely filled with intracellular hyphae before the colonization of adjacent cells. (*g*) The cell wall of the colonized cell is strongly stained with Congo red because of better dye accessibility compared with noncolonized neighbor cells (asterisks). Penetrated cells did not show autofluorescence. (*h*) Intracellular mycelium in mature root tissue. Overlay of bright-field image and fluorescence image. Intracellular hyphae form necks (arrowheads) at sites of cell wall crossing. Fungal structures are visualized by WGA-AF 488. [Scale bars: *a*, 300 μm; *b* and *d*, 10 μm (*c* and *d* are of the same scale); *f–h*, 30 μm.]

Quantitative PCR analysis of *HvBI-1* expression showed it slowly increasing during root development throughout the course of the experiment (Fig. 4*a*). In contrast, when roots were colonized by *P. indica*, *HvBI-1* expression was significantly reduced as compared with noncolonized roots from 7 days after inoculation (dai) onwards (Fig. 4*a*). These data support the idea that *P. indica* interacts with the host cell death machinery for successful development but does not cause plant stress.

To gain evidence for a role of host PCD and requirement of *HvBI-1* down-regulation for fungal success, we overexpressed a functional GFP–HvBI-1 fusion protein in barley under control of the constitutive cauliflower mosaic virus 35S promoter and analyzed fungal development. GFP–HvBI-1 expression was confirmed by PCR and by observation of the fluorescence of GFP–HvBI-1 at the nuclear envelope and in the endoplasmic reticulum in all transgenic plants used for further analysis (Fig. 5, which is published as supporting information on the PNAS web site). Root development in all independent GFP–HvBI-1

barley lines tested was macroscopically indistinguishable from wild type. We microscopically observed development of *P. indica* in GFP–HvBI-1 barley. Fungal epiphytic growth and sporulation were not strongly affected by GFP–HvBI-1. In contrast, invasive inter- and intracellular fungal growth was significantly reduced in GFP–HvBI-1 roots at 20 dai. To quantify the impact of GFP–HvBI-1 on fungal proliferation, the amount of *P. indica* was measured by quantitative PCR. At 20 dai, the relative amount of *P. indica* DNA in transgenic plants was only 20–50%, compared with wild-type plants depending on the transgenic line tested (Fig. 4*b*).

Discussion

P. indica and barley form a mutualistic symbiosis in which the endophyte colonizes the plant root, proliferates by inter- and intracellular growth and produces chlamydospores in dead root tissue. After establishment of the symbiosis the fungus confers improved growth, disease resistance and abiotic stress tolerance
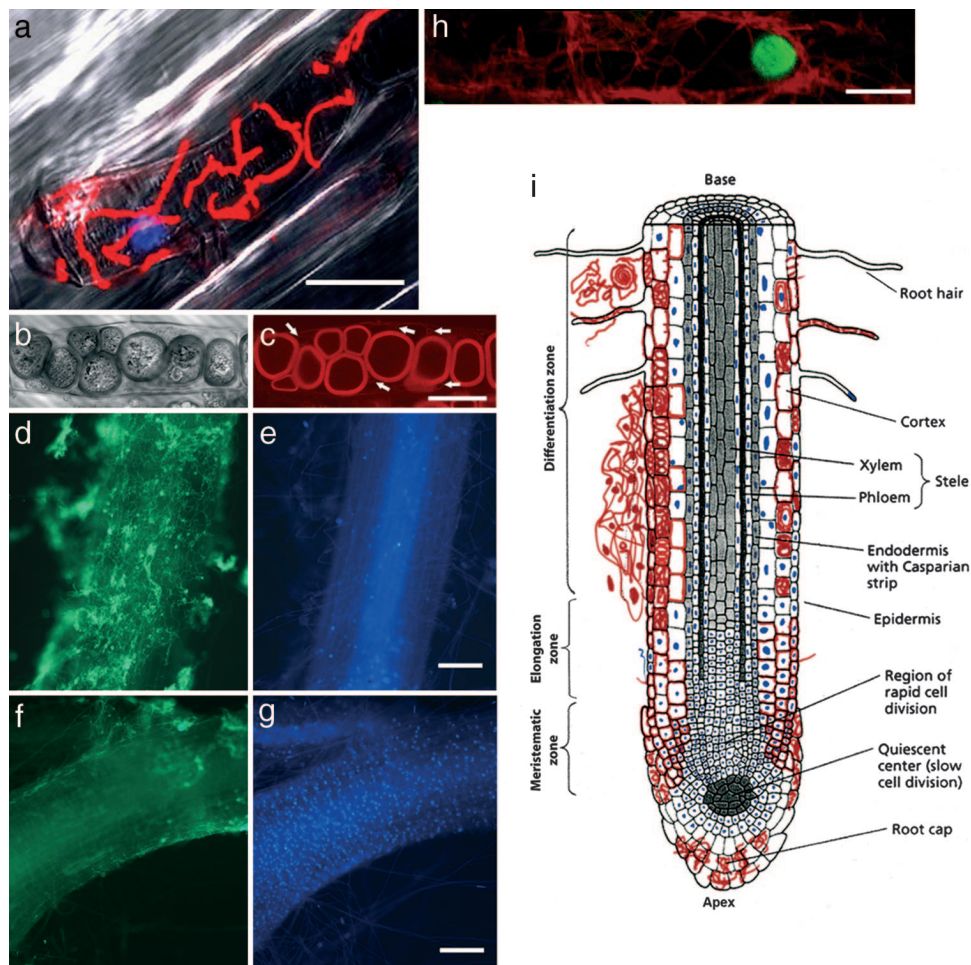
Fig. 3. Association of fungal structures with living and dead cells of the host tissue. (*a*) Fungal hyphae swathe a plant protoplast, which undergoes cytoplasmic shrinkage. Hyphae and nucleus stained with WGA-TMR and DAPI, respectively, are superimposed with the bright-field image. (*b*) Bright-field interference contrast image of chlamydospores in a root cortex cell. (*c*) Fluorescence image of the same cell stained with fuchsin-lactic acid. Arrows indicate hyphae on which the chlamydospores are formed. (*d–g*) Root colonization spatially associated with the absence of intact plant nuclei. Root segments (60 hours after inoculation) double-stained for intact plant nuclei (DAPI; *e* and *g*) and fungal hyphae (WGA-AF 488; *d* and *f*). (*d* and *e*) A root segment heavily colonized by fungal hyphae (*d*) contains only a few DAPI-stained nuclei (*e*). (*f* and *g*) A root segment with minor fungal colonization (*f*) contains a high number of DAPI-stained nuclei (*g*). (*h*) Hyphae swathing a cortical cell protoplast with a TUNEL-positive (green) nucleus. (*i*) Schematic drawing of a *P. indica*-infested root showing the different tissues and the associated colonization pattern, with hyphae depicted in red and DAPI-positive plant nuclei depicted in blue. (Scale bars: *a*, 30 μm; *c*, 10 μm; *d–g*, 300 μm; and *h*, 20 μm.) [Modified from ref. 37 (Copyright 1998, Sinauer, Sunderland, MA).]

to the host plant. Based on the nucLSU sequences our data show that strains of the *S. vermifera* species complex (Sebacinales group B) are closely related to *P. indica* (Fig. 1). These strains yield comparable biological activities in terms of biomass increase and systemic resistance to the biotrophic powdery mildew fungus (Table 1). Hence, the order Sebacinales, of which *P. indica* is considered a model organism, is a source of endophytes with a prospective agronomical impact.

To gain a better understanding of the cellular events leading to the establishment of the mutualistic symbiosis, we microscopically analyzed the interaction of the fungus with the root during the first days of development. After germination of chlamydospores, fungal hyphae grow closely aligned to the topography of rhizodermal cells before penetration of the root at the anticlinal interface of adjacent rhizodermal cell walls (Fig. 2 *b–e*). At such sites, hyphal branching initiates the formation of subepidermal intercellular networks. Intercellular growth is followed by the penetration of rhizodermal cells, which preferentially occurs in differentiated tissue. In young differentiated tissue, single penetrated cells are completely filled with fungal hyphae (Fig. 2 *f* and *g*). Such cells may provide resources for further invasive fungal

growth. Mature root tissue is occupied by a network of intracellular hyphae, whose cell to cell "movement" is indicated by hyphal constrictions ("necks"; see Fig. 2*h*). In either case, fungal colonization proceeds by intra- and intercellular infestation of surrounding tissue and gradually increases with tissue maturation. Further proliferation of fungal hyphae finally leads to the development of extra- and intraradical "mats" of hyphae. At this stage, we visualized a clear spatial association of dead root tissue with strong mycelial growth. Dead tissue is characterized by the absence of intact plant nuclei, which were detectable in adjacent, less infected tissue (Fig. 3 *d–g*). This close association of host cell death with massive fungal growth suggests that the fungus contributes to host cell death. Although *P. indica* can induce cell death in poplar under specific conditions on artificial medium (18), fungal culture filtrate did not show any phytotoxic activity on barley (data not shown). At particular interaction sites, we obtained cytological evidence that the fungus can attack and enwrap living (DAPI-positive) protoplasts (Fig. 3*a*). Because *P. indica* can grow between and penetrate into living cells, we suggest that close association of the fungus with living tissue contributes to host reprogramming and, finally, cell death. The
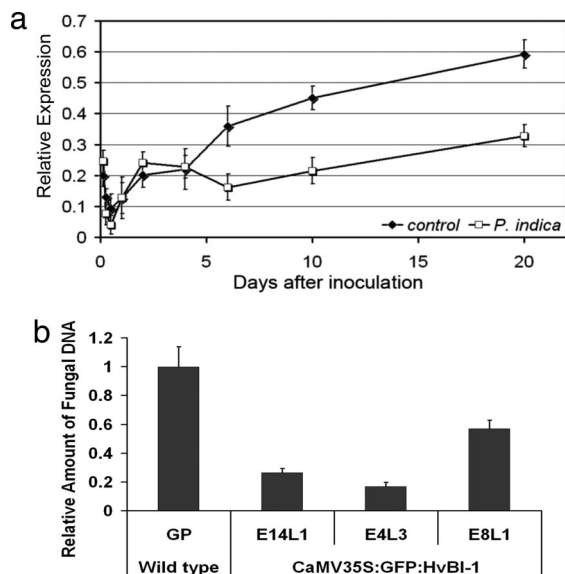
Fig. 4. Influence of HvBI-1 on the development of *P. indica* in barley roots. (*a*) Quantitative PCR analysis of *HvBI-1* expression. As compared with non-colonized roots, expression of the gene is significantly lower from 7 dai onward up to 20 dai. Error bars represent standard deviations. (*b*) The relative amount of *P. indica* DNA in transgenic GFP-HvBI-1 roots was determined at 20 dai. Error bars represent standard deviations. GP represents wild-type plants (Golden Promise). E14L1, E4L3, and E8L1 represent independent transgenic GFP-HvBI-1 GP lines, with five plants tested per line. All three lines were significantly different from the wild type (*P* <0.005, Student's *t* test). Similar results were obtained in three experiments with plants of an independent transgenic GFP-HvBI-1 line.

inter- and intracellular growth pattern indicated that the fungus is also able to digest plant cell walls and we observed the elimination of transverse cell walls of adjoining cortex cells colonized by the fungus and/or filled with spores (data not shown). In summary, these observations indicate the fungus' capacity to attack and enter host tissue and to proliferate and sporulate in dead cells, most notably in the root differentiation zone (Figs. 2*a* and 3*i*). To obtain molecular evidence for a requirement of host cell death regulation, we analyzed the role of the cell death regulator HvBI-1. Although levels of *HvBI-1* mRNA slowly increased during barley root development, *P. indica*-colonized roots showed a significant reduction of *HvBI-1* mRNA levels compared with noncolonized roots from 7 dai onward (Fig. 4*a*). These data suggest a lowered threshold for PCD in endophyte-colonized roots and support the idea that *P. indica* influences intrinsic plant PCD. In barley leaves, *HvBI-1* is strongly expressed in incompatible interactions with the obligate biotrophic leaf pathogen *B. graminis* (15) and may have a role in restricting resistance-associated hypersensitive cell death reactions. The fact that *P. indica* attenuates expression of *HvBI-1* therefore indicates that PCD observed in the interaction with *P. indica* is different from hypersensitive cell death in pathogen defense. It remains to be shown what kind of PCD might be controlled by *P. indica*.

Previous work showed that HvBI-1 has a central role in the outcome of host–pathogen interactions (16, 19, 20). To functionally confirm the role of host PCD and a requirement of *HvBI-1* down-regulation for fungal proliferation, we constitutively overexpressed a GFP–HvBI-1 fusion protein in barley. All transgenic lines showed enhanced resistance to cell death induced by transient expression of mouse BAX in epidermal leaf cells (R. Eichmann, unpublished results). Comparison of the transgenic plants with the respective wild type showed a significant reduction of invasive growth of *P. indica* in GFP–HvBI-1

barley at 20 dai, when fungal proliferation is in a steady state. In contrast, transient overexpression of *HvBI-1* in barley leaf epidermis supported early biotrophic invasion of *B. graminis* into resistant barley (15, 21). Additionally, all GFP–HvBI-1 lines that restricted proliferation of *P. indica* showed enhanced susceptibility to a virulent isolate of *B. graminis*. This effect relied on a lower ability of the plant to stop the fungus by hypersensitive cell death, which is involved in basal barley disease resistance (V. Babaeizad, R. Eichmann, and J.I., unpublished results). Hence, the expression level of HvBI-1 might inhibit or support fungal proliferation depending on the microbial lifestyle. Quantification of *P. indica* confirmed that fungal growth was significantly restricted in GFP–HvBI-1 barley (Fig. 4*b*). Taken together, we provide genetic evidence that *P. indica* requires host cell death for successful proliferation. We suggest that the mutualistic symbiosis between *P. indica* and barley involves a sophisticated regulation of the plant's cell death machinery. The close spatial association of root cell death with massive infestation by *P. indica* might reflect the fungus' success to manipulate host cell PCD. Thereby *P. indica* might take advantage of naturally occurring root cell death in mature parts of the root. However, the main part of the root further develops and is not necrotized when colonized by the fungus.

Conclusion and Perspectives

The mutualistic symbiosis of crop plants and Sebacinales has a great potential for sustainable agriculture. In contrast to AMF, *P. indica* and other members from the same order mediate resistance to root pathogens and systemic resistance to biotrophic leaf pathogens. From an agronomical point of view, it is most promising that *P. indica* can enhance crop yield in cereals (10). Exploitation of endophytic fungi like *P. indica* may, however, not only complement crop production strategies, which presently rely on a high input of fungicides, but additionally may be an eminent source of molecular traits affecting both disease resistance and grain yield in cereals. For future utilization, it is important to gain additional information on effective application strategies (e.g., spore formulation), growth conditions, and the influence of environmental factors. The prospected huge biodiversity in the Sebacinales (11) and the physiological variation between the Sebacinales strains yield the perspective that for a given crop plant an optimal sebacinalean mutualist might become available. This latter notion is supported by the results of our molecular phylogenetic analysis (Fig. 1), which shows that the type of the interaction between Sebacinales and their plant hosts is probably influenced to a greater extent by the plant than by the fungus. Strains of the *S. vermifera* species complex that interacted with barley similar to *P. indica* were originally isolated from Australian orchids (11). In orchid mycorrhizae, however, the fungus invades vital cortical root cells of the host to form intracellular hyphal coils. The strains tested in the present study also are closely related to members of the Sebacinales that form cavendishioid mycorrhizas (14) with certain hemiepiphytic ericads (Fig. 1). In this mycorrhizal association, the fungal partner also predominantly invades vital cortical cells. It is evident that the mutualistic symbiosis between plants and fungi of the Sebacinales is a treasure chest to discover mechanisms to protect plants from biotic and abiotic stresses. Although evidence has been provided that the plant's antioxidant system plays a pivotal role in the *P. indica*-mediated stress tolerance (10), the precise mechanism and underlying signaling pathways remain to be elucidated. In this respect, *P. indica* has another important advantage: In contrast to AMF, *P. indica* colonizes *Arabidopsis*, and our recent results provide evidence that the fungus induces systemic resistance in this model plant similar to the resistance provided to the powdery mildew fungus in barley (our unpublished data). The power of the *Arabidopsis* signal transduction mutants available and reverse genetics will soon accelerate

disclosure of the molecular basis of the symbiosis and its beneficial effects on the host. Despite this perspective, differences in signaling pathways relevant for agronomically important traits exist between *Arabidopsis* and cereals, justifying strong emphasis on future cereal research.

Materials and Methods

Plant and Fungal Material and Plant Inoculation. Barley (*Hordeum vulgare* L.) cultivar Golden Promise was obtained from Jörn Pons-Kühnemann (University of Giessen, Giessen, Germany). *P. indica* isolate *WP2* was propagated as described (10). *S. vermifera* isolates (culture collection numbers; see Table 1) were propagated in MYP medium (aqueous solution of 7 g/liter malt extract, 1 g/liter peptone and 0.5 g/liter yeast extract).

For inoculation, barley kernels were sterilized with 6% sodium hypochloride, rinsed in water, and germinated for 2 days. Subsequently, seedling roots were immersed in an aqueous solution of 0.05% Tween-20 containing 5×10^5 ml^{-1} *P. indica* chlamydospores or homogenized mycelial solution (1 g/ml) of *S. vermifera*, respectively. Inoculated seedlings were grown in a 2:1 mixture of expanded clay (Seramis; Masterfoods, Verden, Germany) and Oil Dri (Damolin, Mettmann, Germany) (10).

Molecular Phylogenetic Analysis. We used nuclear DNA sequences coding for the 5′ terminal domain of the ribosomal large subunit to estimate the phylogenetic position of the Sebacinales strains used in the present study. An alignment covering a representative sampling of nucLSU sequences available for this fungal group was constructed with MAFFT 5.850 (22). The alignment was analyzed by using heuristic maximum likelihood as implemented in PHYML 2.4.4 (23), with a general time-reversible model of nucleotide substitution and additionally assuming a percentage of invariant sites and Γ-distributed substitution rates at the remaining sites (GTR+I+G; the Γ distribution approximated with four discrete rate categories), starting from a BIONJ tree (24). All model parameters were estimated by using maximum likelihood. Branch support was inferred from 1,000 replicates of nonparametric maximum-likelihood bootstrapping (25), with model parameters estimated individually for each bootstrap replicate. Additionally we performed a Bayesian Markov chain Monte Carlo analysis with MrBayes 3.1 (26). We ran two independent Markov chain Monte Carlo analyses, each involving four incrementally heated chains over two million generations, using the GTR+I+G model of nucleotide substitution and starting from random trees. Trees were sampled every 100 generations, resulting in an overall sampling of 20,000 trees per run, from which the first 5,000 trees of each run were discarded (burn in). The remaining 15,000 trees sampled in each run were pooled and used to compute a majority rule consensus tree to get estimates for the posterior probabilities. Stationarity of the process was controlled by using the Tracer program (27).

Generation of Transgenic Barley Plants. For constitutive overexpression and for tagging expression, we cloned a cDNA fusion of GFP and *HvBI-1* by digestion of pGY1-CaMV35S::GFP–HvBI-1 (15, 21) into appropriate sites of the binary vector pLH6000 (DNA Cloning Service, Hamburg Germany), which was then introduced into *Agrobacterium tumefaciens* strain AGL1 (28) to transform barley cultivar Golden Promise as described (29, 30). PCR analysis was used to confirm integration of the transfer DNA. The GFP reporter was visualized with either a standard fluorescence microscope or a confocal laser scanning microscope as described below.

Root Fixation, Staining and Microscopy, and DAPI Staining. Root segments were fixed as described in ref. 31, with noted exceptions. Fixed root segments were transferred to an enzyme solution containing 10 mg/ml driselase and chitinase, 16 mg/ml

β-D-glucanase (InterSpex Products, San Mateo, CA) and 1 mg/ml BSA (Sigma, St. Louis, MO) dissolved in 25 mM phosphate buffer (PB) (4.0 g of NaCl/0.1 g of KCl/0.7 g of Na$_2$HPO4 2H$_2$O/0.1 g of KH$_2$PO4 in 500 ml water, pH 6.8) at room temperature for 15 min. After rinsing in PB, roots were further treated with 0.5% Triton X-100 in PB for 10 min. After additional rinsing in PB, plant nuclei were stained with 1 μg/ml DAPI for 30 min. During incubation, segments were vacuum-infiltrated three times for 1 min at 25 mmHg (1 mmHg = 133 Pa) and then rinsed with PB. Additionally, root material was stained with WGA-AF 488 as described below. All segments were analyzed with an Axioplan 2 microscope (excitation 365 nm and emission 420–540 nm; Zeiss, Jena, Germany).

A TUNEL assay was performed using an *in situ* cell death detection kit (Fluorescein; Roche Applied Science, Penzberg, Germany) according to the instruction manual. Root segments were fixed as described above. In addition, root segments were dehydrated and dewaxed by passage for 15 min through series of increasing concentrations of ethanol in water (from 10% to 100% in 10% increments) and back from 100% to 0% in 10% increments). Subsequently, segments were incubated in 50 μl of TUNEL reaction mixture. Grade 1 DNase I-treated roots were used as positive controls. Solutions were vacuum-infiltrated as described above and incubated for 60 min at 37°C in humidified atmosphere in the dark. Subsequently, segments were washed and transferred to 1× PB (pH 7.4) for destaining. Destained segments were counterstained with wheat germ agglutinin-tetramethylrhodamine (WGA-TMR) as described below. TUNEL-positive nuclei were excited at 488 nm and detected at 505–540 nm. Fluorescein diacetate vitality staining and actin staining of barley root was performed according to refs. 32 and 33, respectively.

Staining of *P. indica* in Root Tissue. Hyphae in root segments were either stained by 0.01% acid fuchsin-lactic acid (10) or with the chitin-specific dyes WGA-AF 488 and WGA-TMR (Molecular Probes, Karlsruhe, Germany). Depending on the studies, root material was either fixed for some experiments, dehydrated as described above, or transferred to trichloroacetic acid fixation solution [0.15% (wt/vol) trichloroacetic acid in 4:1 (vol/vol) ethanol/chloroform]. Subsequently, segments were incubated at room temperature for 10 min in 1× PBS (pH 7.4) containing each respective dye at 10 μg/ml. During incubation, segments were vacuum-infiltrated three times for 1 min at 25 mmHg. After rinsing with 1× PBS (pH 7.4), segments were mounted on glass slides. In cases that Congo red (Merck, Darmstadt, Germany) was used for counterstaining, it was added to WGA-AF 488 staining solution at a final concentration of 10 μg/ml. Confocal fluorescence images were recorded on a multichannel TCS SP2 confocal microscope (Leica, Bensheim, Germany). WGA-AF 488 was excited with a 488-nm laser line and detected at 505–540 nm. WGA-TMR was excited with a 543-nm laser line and detected at 560–630 nm. All segments that were analyzed with an Axioplan 2 microscope were either excited at 470/20 nm and detected at 505–530 nm for WGA-AF 488 or excited at 546/12 nm and detected at 590 nm for Congo red.

Genomic DNA Isolation, Real-Time PCR, and Transcript Analysis. The degree of root colonization was determined by using the $2^{-\Delta Ct}$ method (34). Cycle threshold (Ct) values were generated by subtracting the raw Ct values of the *P. indica* internal transcribed spacer or *Tef* gene (35) from the raw Ct values of plant-specific ubiquitin.

Roots were harvested, frozen, and ground in liquid nitrogen, and genomic DNA was isolated from ≈100 mg of root powder with the Plant DNeasy kit (Qiagen, Hilden, Germany) according to the manufacturer's instructions. For quantitative PCR, 5–10 ng of total DNA was used. Amplifications were performed in 20

μl of SYBR green JumpStart *Taq* ReadyMix (Sigma–Aldrich, Munich, Germany) with 350 nM oligonucleotides, using an Mx3000P thermal cycler (Stratagene, La Jolla, CA). After an initial activation step at 95°C for 7 min, 40 cycles (94°C for 30 s, 60°C for 30 s, 72°C for 30 s, and 82°C for 15 s) were performed, and a single fluorescent reading was obtained after the 82°C step of each cycle. A melting curve was determined at the end of cycling to ensure amplification of only a single PCR product. Ct values were determined with the Mx3000P V2 software supplied with the instrument.

For quantitative two-step RT-PCR, 2 μg of total RNA were reverse-transcribed to first-strand cDNA with the iScript cDNA synthesis kit (Bio-Rad, Hercules, CA). Aliquots of 20 ng of first-strand cDNA were subsequently used as a template for quantitative PCR with gene-specific primers. The plant-specific ubiquitin gene served as a control for constitutive gene expression in roots. Ubiquitin expression was consistent after inoculation with *P. indica* when compared with the amount of 18S ribosomal RNA. Specific PCR conditions were as described above, and comparative expression levels ($2^{-\Delta Ct}$) were calculated according to ref. 36. Expression levels are relative to the level of ubiquitin expression, which was constant in all RNA samples used and was set to 1. Values are the means of four samples of one biological experiment (infected roots) assayed by quantitative PCR in triplicate. The oligonucleotides used were as follows: ubiquitin (accession no. M60175), 5′-CAGTAGTG-GCGGTCGAAGTG-3′ and 5′-ACCCTCGCCGACTACAA-CAT-3′; *P. indica* Tef (accession no. AJ249911) 5′-ACCGTCT-TGGGGTTGTATCC-3′ and 5′-TCGTCGCTGTCAA-CAAGATG-3′; Bax inhibitor-1 (accession no. AJ290421) 5′-GTCCCACCTCAAGCTCGTTT-3′ and 5′-ACCCTGTCAC-GAGGATGCTT-3′; and *P. indica* ITS (accession no. AF 019636) 5′-CAACACATGTGCACGTCGAT-3′ and 5′-CCAATGTGCATTCAGAACGA-3′

1. Kogel KH, Franken P, Hückelhoven R (2006) *Curr Opin Plant Biol* 9:358–363.
2. Harrison MJ (2005) *Annu Rev Microbiol* 59:19–42.
3. Borowicz VA (2001) *Ecology* 82:3057–3068.
4. Arnold AE, Mejia LC, Kyllo D, Rojas EI, Maynard Z, Robbins N, Herre EA (2003) *Proc Natl Acad Sci USA* 100:15649–15654.
5. Müller CB, Krauss J (2005) *Curr Opin Plant Biol* 8:450–456.
6. Garcia-Garrido JM, Ocampo JA (2002) *J Exp Bot* 53:1377–1386.
7. Grunwald U, Nyamsuren O, Tamasloukht M, Lapopin L, Becker A, Mann P, Gianinazzi-Pearson V, Krajinski F, Franken P (2004) *Plant Mol Biol* 55:553–566.
8. Schulz B, Boyle C (2005) *Mycol Res* 109:661–686.
9. Verma S, Varma A, Rexer K-H, Hassel A, Kost G, Sarabhoy A, Bisen P, Bütehorn B, Franken P (1998) *Mycologia* 90:896–903.
10. Waller F, Achatz B, Baltruschat H, Fodor J, Becker K, Fischer M, Heier T, Hückelhoven R, Neumann C, von Wettstein D, *et al*. (2005) *Proc Natl Acad Sci USA* 102:13386–13391.
11. Weiss M, Selosse M-A, Rexer K-H, Urban A, Oberwinkler F (2004) *Mycol Res* 108:1003–1010.
12. Varma A, Verma S, Sudha, Sahay N, Bütehorn B, Franken P (1999) *Appl Environ Microbiol* 65:2741–2744.
13. Peškan-Berghöfer T, Shahollari B, Giong PH, Hehl S, Markert C, Blanke V, Kost G, Varma A, Oelmüller R (2004) *Physiol Plant* 122:465–477.
14. Setaro S, Weiss M., Oberwinkler F, Kottke I (2006) *New Phytologist* 169:355–365.
15. Hückelhoven R, Dechert C, Kogel K-H (2003) *Proc Natl Acad Sci USA* 100:5555–5560.
16. Hückelhoven R (2004) *Apoptosis* 9:299–307.
17. Chae HJ, Kim HR, Xu C, Bailly-Maitre B, Krajewska M, Krajewski S, Banares S, Cui J, Digicaylioglu M, Ke N, *et al*. (2004) *Mol Cell* 15:355–366.
18. Kaldorf M, Koch B, Rexer K-H, Kost G, Varma A (2005) *Plant Biol* 7:210–218.
19. Imani J, Baltruschat H, Stein E, Jia G, Vogelsberg J, Kogel K-H, Hückelhoven R (2006) *Mol Plant Pathol* 7:279–284.
20. Watanabe N, Lam E (2006) *Plant J* 45:884–894.
21. Eichmann R, Schultheiss H, Kogel K-H, Hückelhoven R (2004) *Mol Plant–Microbe Interact* 17:484–490.
22. Katoh K, Misawa K, Kuma K, Miyata T (2002) *Nucleic Acids Res* 30:3059–3066.
23. Guindon S, Gascuel O (2003) *Syst Biol* 52:696–704.
24. Gascuel O (1997) *Mol Biol Evol* 14:685–695.
25. Felsenstein J (1985) *Evolution* 39:783–791.
26. Ronquist F, Huelsenbeck JP (2003) *Bioinformatics* 19:1572–1574.
27. Rambaut A, Drummond A. (2006) Tracer, MCMC Trace Analysis Tool (University of Oxford, Oxford).
28. Lazo GR, Stein PA, Ludwig RA (1991) *Biotechnology (NY)* 9:963–967.
29. Tingay S, McElroy D, Kalla R, Fieg S, Wang M, Thornton S, Brettell R (1997) *Plant J* 11(6):1369–1376.
30. Matthews PR, Wang MB, Waterhouse PM, Thornton S, Fieg SJ, Gubler F, Jacobsen JV (2001) *Mol Breed* 7:195–202.
31. Opalski KS, Schultheiss H, Kogel K-H, Hückelhoven R (2005) *Plant J* 41:291–303.
32. Pan JW, Zhu MY, Chen H (2001) *Environ Exp Bot* 46:71–79.
33. Vitha S, Baluska F, Mews M, Volkmann D (1997) *J Histochem Cytochem* 45(1):89–95.
34. Livak KJ, Schmittgen TD (2001) *Methods* 25:402–408.
35. Bütehorn B, Rhody D, Franken P (2000) *Plant Biol* 2:687–692.
36. Wulf A, Manthey K, Doll J, Perlick AM, Linke B, Bekel T, Meyer F, Franken P, Kuster H, Krajinski F (2003) *Mol Plant–Microbe Interact* 16(4):306–314.
37. Taiz L, Zeiger E (1998) *Plant Physiology* (Sinauer, Sunderland, MA), p 119.